Monthly Notices
of the
ROYAL ASTRONOMICAL SOCIETY

Mon. Not. R. Astron. Soc. (2012) doi:10.1111/j.1365-2966.2011.20363.x

The evolution stage and massive disc of the interacting binary V 393 Scorpii

R. E. Mennickent,[1⋆] G. Djurašević,[2,3] Z. Kołaczkowski[1,4] and G. Michalska[1,4]

[1] *Universidad de Concepción, Departamento de Astronomía, Casilla 160-C, Concepción, Chile*
[2] *Astronomical Observatory, Volgina 7, 11060 Belgrade 38, Serbia*
[3] *Isaac Newton Institute of Chile, Yugoslavia Branch, Serbia*
[4] *Instytut Astronomiczny Uniwersytetu Wroclawskiego, Kopernika 11, 51-622 Wroclaw, Poland*

Accepted 2011 December 9. Received 2011 December 9; in original form 2011 September 8

ABSTRACT

V 393 Scorpii is a bright Galactic Double Periodic Variable showing a long photometric cycle of ≈253 d. We present new *VIJK* photometric time series for V 393 Scorpii along with the analysis of All Sky Automated Survey (ASAS) *V*-band photometry. We disentangled all light curves into the orbital and long-cycle components. The ASAS *V*-band *orbital* light curve was modelled with two stellar components plus a circumprimary optically thick disc assuming a semi-detached configuration. We present the results of this calculation, giving physical parameters for the stars and the disc, along with general system dimensions. Our results are in close agreement with those previously found by Mennickent et al. from infrared (IR) spectroscopy and the modelling of the spectral energy distribution. The stability of the orbital light curve suggests that the stellar plus disc configuration remains stable during the long cycle. Therefore, the long cycle should be produced by an additional variable and not-eclipsed emitting structure. We discuss the evolutionary stage of the system finding the best match with one of the evolutionary models of van Rensbergen et al. According to these models, the system is found to be after an episode of fast mass exchange that transferred 4 $M_\odot$ from the donor to the gainer in a period of 400 000 years. We argue that a significant fraction of this mass has not been accreted by the gainer but remains in an optically thick *massive* (∼2 $M_\odot$) disc-like surrounding pseudo-photosphere whose luminosity is not driven by viscosity but probably by reprocessed stellar radiation. Finally, we provide the result of our search for Galactic Double Periodic Variables and briefly discuss the outliers β Lyr and *RX* Cas.

Key words: stars: early-type – stars: emission-line, Be – stars: evolution – stars: mass-loss – stars: variables: general.

1 INTRODUCTION

V 393 Scorpii is one of the Galactic Double Periodic Variables (DPVs), a group of interacting binaries showing a long photometric cycle lasting roughly 33 times the orbital period (Mennickent et al. 2003; Mennickent & Kołaczkowski 2009; Michalska et al. 2010; Poleski et al. 2010). DPVs have been interpreted as semi-detached interacting binaries with ongoing cyclic episodes of mass loss into the interstellar medium (Mennickent et al. 2008; Mennickent & Kołaczkowski 2010). The 253-d long photometric cycle of V 393 Scorpii was discovered by Pilecki & Szczygiel (2007) after inspection of the All Sky Automated Survey (ASAS) catalogue (Pojmanski 1997) for eclipsing binaries with additional variability. The data obtained with the *International Ultraviolet Explorer* (IUE) satellite were studied by Peters (2001) who found evidence for a hot temperature region produced by the tangential impact of the gas stream into the gainer photosphere. This region should be the origin of the superionized lines observed in the UV, like N v, C iv and Si iv, that are likely produced by resonance scattering in a plasma of temperature $T \sim 10^5$ K and electron density $N_e \sim 10^9$ cm^{-3} (Peters & Polidan 1984). The star was also studied by means of multi-epoch high-resolution IR spectroscopy by Mennickent et al. (2010, hereafter M10), who also studied broad-band photometry and IUE ultraviolet spectra. After summarizing the available literature of this object, these authors argued for a semi-detached B3 + F0 binary with masses 8 $M_\odot$ and 2 $M_\odot$ for the gainer and donor (hereafter also called primary and secondary, respectively) and orbital separation of 35 $R_\odot$. Most remarkably, M10 found evidence for large mass loss through the Lagrangian L3 point during epochs of long-cycle minimum and claim that their observations suggest that the mass loss producing the long cycle is probably concentrated in equatorial regions.

⋆E-mail: rmennick@astro-udec.cl

Table 1. Summary of photometric data analysed in this paper. ASAS data can be found at http://www.astrouw.edu.pl/asas/.

Observatory	Telescope	Filters	N	HJD range (−245 0000)
La Silla	REM 60 cm	*V*	359	4498.8391–5372.6688
La Silla	REM 60 cm	*I*	340	4498.8402–5391.7978
La Silla	REM 60 cm	*J*	210	4498.8393–5362.8939
La Silla	REM 60 cm	*K*	169	4502.8541–5369.8908
Las Campanas	ASAS array	*V*	903	1950.8740–4973.8121

In this paper we refine stellar and system parameters of V 393 Scorpii by fitting the light curve with a multi-component model including a stationary circumprimary disc. A detailed report of the observations used in this paper is given in Section 2; our results are presented in Section 3; a detailed discussion of these results is given in Section 4 and our conclusions are presented in Section 5.

2 OBSERVATIONS

We obtained *V, I, J, K* band images with the robotic 60-cm Rapid Eye Mount (REM) telescope operated at La Silla, Chile, during three seasons in 2008–2010. Bias and flat calibration images were regularly obtained, and de-biasing and flat-fielding for all science images were done with standard photometric IRAF[1] tasks. Instrumental magnitudes were calculated using aperture photometry and also by applying the differential image analysis technique (DIA; e.g. Allard & Lupton 1998). Differential magnitudes were calculated between the target and nearby stars used as comparison stars. The DIA technique provided the less noisy light curves and are shown in this paper. We also analysed *V*-band magnitudes available in the public ASAS archive.[2] Typical one-sigma error for ASAS and REM photometry is 0.03 and 0.05 mag, respectively. This is the kind of statistical error provided in the rest of the paper for some modelled or fitting quantities. A summary of all photometric observations analysed in this paper is given in Table 1.

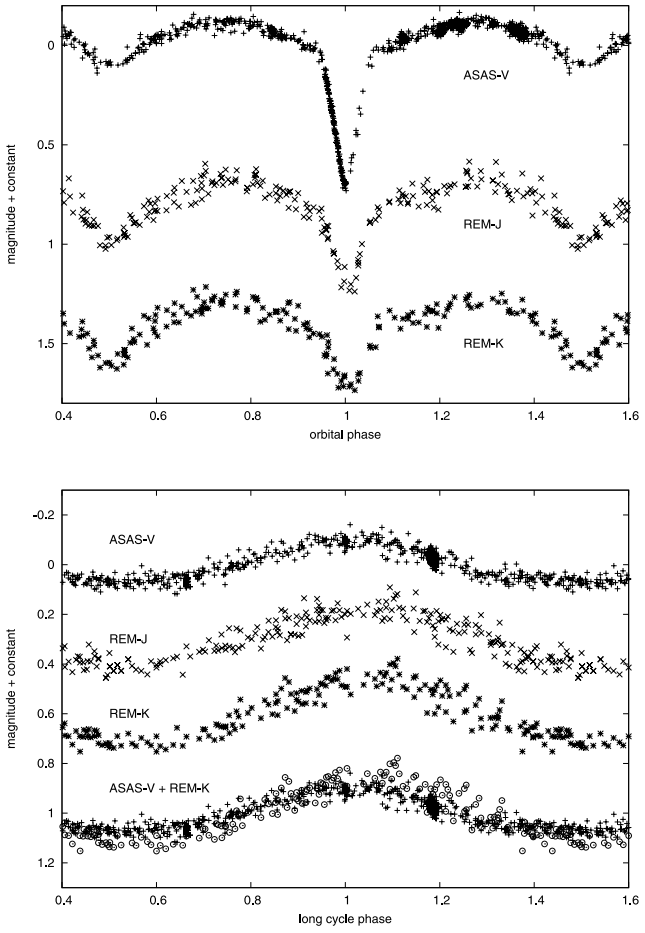

Figure 1. Orbital light curve (up) and long-cycle light curve (down) of V 393 Scorpii at three bandpasses. Ephemeris is given in the text. In the lower light curve circles represent REM-*K* and pluses ASAS-*V* data.

3 RESULTS

3.1 Light-curve disentangling

In this paper we use the ephemeris for the main orbital photometric minimum provided by Kreiner (2004), namely $T_o = 2\,45\,2507.7800 + 7.712\,5772E$. We separated the light curve of V393 Sco into a long- and a short-period component. For that we used an algorithm especially designed to disentangle multi-periodic light curves through the analysis of their Fourier component amplitudes. The method works as follows. A main frequency f_1 (usually the orbital one) is found with a period searching algorithm applied to the light curve. A least-square fit is applied to the light curve considering a fitting function consisting of a sum of sine functions of variable amplitude and phases representing the main frequency and their additional significant harmonics. After this first fit, the residuals are inspected for a new periodicity f_2 (the long periodicity in DPVs). This new periodicity and their harmonics are included in the new fitting procedure. Finally, we obtain the best representation for the light curve based on a sum of Fourier components of frequency f_1, f_2 and their significant harmonics. Data residuals with respect to the second and first theoretical light curves form the orbital and long-cycle photometric series, respectively.

This deconvolution method was applied to the light curves of V 393 Sco at the observed bandpasses yielding a unique solution consisting of the orbital light curve plus an additional smooth variability with a period of 253 d. A phase dispersion minimization analysis (Stellingwerf 1978) of combined ASAS-*V* and REM-*V* data yielded for the long cycle the following ephemeris for the light curve maximum:

$$\mathrm{HJD}_{\mathrm{max,long}} = 245\,2522(\pm1) + 253(\pm4) * E. \quad (1)$$

Inspection of the orbital and long light curves at different bandpasses reveals that (Fig. 1): (i) the rounded shape of the orbital light curves at quadratures is consistent with a close binary showing proximity effects, (ii) the system shows smooth long-cycle variability with larger amplitude in redder bandpasses. The amplitudes of this long variability in the *V*, *I*, *J* and *K* bands, derived from sinus fits to the REM data, are 0.177 ± 0.003, 0.240 ± 0.004, 0.231 ± 0.003 and 0.263 ± 0.003 mag, respectively, and (iii) *V* and *K* light curves look different, the maximum of the latter seems to be delayed by $\Delta\Phi_l \approx 0.05$ with respect to the former.

[1] IRAF is distributed by the National Optical Astronomy Observatories, which are operated by the Association of Universities for Research in Astronomy, Inc., under cooperative agreement with the National Science Foundation.
[2] www.astrouw.edu.pl/asas/

The orbital light curve was examined with the program sc Period04.[3] We calculated the error in the main frequency of the fit to the orbital light curve. The error consistently given by Monte Carlo simulations and the method of least squares is 4×10^{-7} Hz. This means that the period could drift at most by 4.76×10^{-5} d in 3023 d (the ASAS-*V* data set time baseline). This implies that a constant orbital period change if present should be less than 0.5 seconds per year.

3.2 Model for a circumprimary optically thick disc

Here we give a brief description of the disc model that we apply to V 393 Sco.

The basic elements of the binary system model with a plane-parallel disc and the corresponding light-curve synthesis procedure are described in detail by Djurašević (1992, 1996).

We assume that the disc in V 393 Sco is optically and geometrically thick. The disc edge is approximated by a cylindrical surface. In the current version of the model (Djurašević et al. 2010), the thickness of the disc can change linearly with radial distance, allowing the disc to take a conical shape (convex, concave or plane-parallel). The geometrical properties of the disc are determined by its radius (R_d), its thickness at the edge (d_e) and the thickness at the centre (d_c).

The cylindrical edge of the disc is characterized by its temperature, T_d, and the conical surface of the disc by a radial temperature profile obtained by modifying the temperature distribution proposed by Zola (1991):

$$T(r) = T_\mathrm{d} + (T_\mathrm{h} - T_\mathrm{d}) \left[1 - \left(\frac{r - R_\mathrm{h}}{R_\mathrm{d} - R_\mathrm{h}} \right) \right]^{a_\mathrm{T}}. \quad (2)$$

We assume that the disc is in physical and thermal contact with the gainer, so the inner radius and temperature of the disc are equal to the temperature and radius of the star ($R_\mathrm{h}, T_\mathrm{h}$). The temperature of the disc at the edge (T_d) and the temperature exponent (a_T), as well as the radii of the star (R_h) and of the disc (R_d) are free parameters, determined by solving the inverse problem.

The model of the system is refined by introducing active regions on the edge of the disc. The active regions have higher local temperatures so their inclusion results in a non-uniform distribution of radiation. The model includes two such active regions: a hotspot (HS) and a bright spot (BS). These regions are characterized by their temperatures $T_\mathrm{hs,bs}$ angular dimensions $\theta_\mathrm{hs,bs}$ and longitudes $\lambda_\mathrm{hs,bs}$. These parameters are also determined by solving the inverse problem.

Due to the infall of an intensive gas-stream, the disc surface in the region of the HS becomes deformed as the material accumulates at the point of impact, producing a local deviation of radiation from the uniform azimuthal distribution. In the model, this deviation is described by the angle θ_rad between the line perpendicular to the local disc edge surface and the direction of the HS maximum radiation in the orbital plane.

The second spot in the model, i.e. the BS, approximates the spiral structure of an accretion disc, predicted by hydrodynamical calculations (Heemskerk 1994). The tidal force exerted by the donor star causes a spiral shock, producing one or two extended spiral arms in the outer part of the disc. The BS can also be interpreted as a region where the disc significantly deviates from the circular shape.

[3] http://www.univie.ac.at/tops/period04/

3.3 Results of the *V*-band light-curve fitting

The light-curve fitting was performed using the inverse-problem solving method (Djurašević 1992) based on the simplex algorithm, and the model of a binary system with a disc described in the previous section. To obtain reliable estimates of the system parameters, a good practice is to restrict the number of free parameters by fixing some of them to values obtained from independent sources. Thus we fixed the spectroscopic mass ratio to $q = 0.25$ and the donor temperature to $T_2 = 7900$ *K*, based on our spectroscopic study (Mennickent et al., in preparation). In addition, we set the gravity darkening coefficient and the albedo of the gainer and the donor to $\beta_\mathrm{h,c} = 0.25$ and $A_\mathrm{h,c} = 1.0$ in accordance with von Zeipel's law for radiative shells and complete re-radiation (Von Zeipel 1924). The limb-darkening for the components was calculated in the way described by Djurašević et al. (2010).

We treated the rotation of the donor as synchronous ($f_\mathrm{c} = 1.0$) since it is assumed that it has filled its Roche lobe (i.e. the filling factor of the donor was set to $F_\mathrm{c} = 1.0$). In the case of the gainer, however, the accreted material from the disc is expected to transfer enough angular momentum to increase the rate of the gainer up to the critical velocity as soon as even a small fraction of the mass has been transferred (Packet 1981; de Mink, Pols & Glebbeek 2007). This means that the gainer fills its corresponding non-synchronous Roche lobe for the star rotating in the critical regime, and its dimensions and the amount of rotational distortion are uniquely determined by the factor of non-synchronous rotation, which is the ratio between the actual and the Keplerian angular velocity. For V 393 Scorpii we assumed critical rotation for the gainer, i.e. $f_\mathrm{h} = 14.6$ (Model A) but also calculated a model using synchronous rotation (Model B) to estimate the effect of the gainer velocity in the system parameters.

The results of the light-curve analysis based on the described model of V 393 Sco given in Table 2 basically confirm our solution for the stellar parameters given in M10, based on IR spectroscopy and the modelling of the spectral energy distribution. Furthermore, now we obtain a more realistic R_h value. Our results obtained considering synchronous rotation for the gainer do not differ much from the critical rotational case. The fit and stellar and disc dimensions are illustrated in Fig. 2. We note that residuals show no dependence on orbital or long-cycle phases.

We find that the best-fitting model of V 393 Sco contains an optically and geometrically thick disc around the hotter, more massive gainer star. With a radius of $R_\mathrm{d} \approx 9.7\,\mathrm{R}_\odot$, the disc is more than twice as large as the central star ($R_\mathrm{h} \approx 4.4\,\mathrm{R}_\odot$). The disc has a moderately convex shape, with central thickness of $d_\mathrm{c} \approx 2.1\,\mathrm{R}_\odot$ and the thickness at the edge of $d_\mathrm{e} \approx 1.3\,\mathrm{R}_\odot$. The temperature of the disc increases from $T_\mathrm{d} = 8600$ K at its edge, to $T_\mathrm{h} = 16600$ K at the inner radius, where it is in thermal and physical contact with the gainer. The temperature profile exponent a_T in equation (1) is 4.5; this means that the effective temperature of the disc is significantly higher than the temperature at its edge.

We were able to model the asymmetry of the light curve very precisely by incorporating two regions of enhanced radiation on the disc: the HS and the BS. The HS is situated at longitude $\lambda_\mathrm{hs} \approx 320^\circ$, roughly between the components of the system, at the place where the gas stream falls on to the disc. The longitude λ is measured clockwise (as viewed from the direction of the $+Z$-axis, which is orthogonal to the orbital plane) with respect to the line connecting the star centres ($+X$-axis), in the range 0°–360°. The temperature of the HS is approximately 20 per cent higher than the disc edge temperature, i.e. $T_\mathrm{hs} \approx 10\,300$ K. The HS can be interpreted as a

Table 2. Results of the analysis of V 393 Sco *V*-filter light curve obtained by solving the inverse problem for the Roche model with a disc around the more-massive (hotter) component in critical rotation regime (Model A) and synchronous rotational regime (Model B).

Quantity	Model A	Quantity	Model A	Quantity	Model B	Quantity	Model B
n	2268	$\mathcal{M}_{\rm h}(\mathcal{M}_\odot)$	7.8 ± 0.2	n	2268	$\mathcal{M}_{\rm h}(\mathcal{M}_\odot)$	7.8 ± 0.5
$\Sigma(\mathrm{O-C})^2$	0.5638	$\mathcal{M}_{\rm c}(\mathcal{M}_\odot)$	2.0 ± 0.2	$\Sigma(\mathrm{O-C})^2$	0.5621	$\mathcal{M}_{\rm c}(\mathcal{M}_\odot)$	2.0 ± 0.2
$\sigma_{\rm rms}$	0.0157	$\mathcal{R}_{\rm h}(\mathrm{R}_\odot)$	4.4 ± 0.2	$\sigma_{\rm rms}$	0.0157	$\mathcal{R}_{\rm h}(\mathrm{R}_\odot)$	4.1 ± 0.2
$i(^\circ)$	80.0 ± 0.2	$\mathcal{R}_{\rm c}(\mathrm{R}_\odot)$	9.4 ± 0.3	$i(^\circ)$	79.9 ± 0.2	$\mathcal{R}_{\rm c}(\mathrm{R}_\odot)$	9.4 ± 0.3
$F_{\rm d}$	0.55 ± 0.04	$\log g_{\rm h}$	4.0 ± 0.1	$F_{\rm d}$	0.51 ± 0.04	$\log g_{\rm h}$	4.1 ± 0.1
$T_{\rm d}$(K)	8600 ± 600	$\log g_{\rm c}$	2.8 ± 0.1	$T_{\rm d}$(K)	8300 ± 600	$\log g_{\rm c}$	2.8 ± 0.1
$d_{\rm e}(a_{\rm orb})$	0.04 ± 0.01	$M^{\rm h}_{\rm bol}$	-3.0 ± 0.2	$d_{\rm e}(a_{\rm orb})$	0.04 ± 0.01	$M^{\rm h}_{\rm bol}$	-2.9 ± 0.3
$d_{\rm c}(a_{\rm orb})$	0.06 ± 0.01	$M^{\rm c}_{\rm bol}$	-1.4 ± 0.1	$d_{\rm c}(a_{\rm orb})$	0.08 ± 0.01	$M^{\rm c}_{\rm bol}$	-1.4 ± 0.1
$a_{\rm T}$	4.5 ± 0.5	$a_{\rm orb}(\mathrm{R}_\odot)$	35.1 ± 0.3	$a_{\rm T}$	4.4 ± 0.5	$a_{\rm orb}(\mathrm{R}_\odot)$	35.1 ± 0.5
$f_{\rm h}$	14.6 ± 0.8	$\mathcal{R}_{\rm d}(\mathrm{R}_\odot)$	9.7 ± 0.3	$f_{\rm h}$	1.00	$\mathcal{R}_{\rm d}(\mathrm{R}_\odot)$	9.1 ± 0.5
$F_{\rm h}$	1.00	$\mathrm{d_e}(\mathrm{R}_\odot)$	1.3 ± 0.3	$F_{\rm h}$	0.25 ± 0.01	$\mathrm{d_e}(\mathrm{R}_\odot)$	1.4 ± 0.3
$T_{\rm h}$(K)	$16\,600 \pm 500$	$\mathrm{d_c}(\mathrm{R}_\odot)$	2.1 ± 0.4	$T_{\rm h}$(K)	16800 ± 500	$\mathrm{d_c}(\mathrm{R}_\odot)$	2.8 ± 0.5
$A_{\rm hs} = T_{\rm hs}/T_{\rm d}$	1.2 ± 0.1			$A_{\rm hs} = T_{\rm hs}/T_{\rm d}$	1.3 ± 0.1		
$\theta_{\rm hs}(^\circ)$	19.0 ± 2.0			$\theta_{\rm hs}(^\circ)$	18.5 ± 2.0		
$\lambda_{\rm hs}(^\circ)$	324.0 ± 6.0			$\lambda_{\rm hs}(^\circ)$	325.0 ± 6.0		
$\theta_{\rm rad}(^\circ)$	-5.0 ± 5.0			$\theta_{\rm rad}(^\circ)$	-5.0 ± 5.0		
$A_{\rm bs} = T_{\rm bs}/T_{\rm d}$	1.2 ± 0.1			$A_{\rm bs} = T_{\rm bs}/T_{\rm d}$	1.3 ± 0.1		
$\theta_{\rm bs}(^\circ)$	33.0 ± 6.0			$\theta_{\rm bs}(^\circ)$	29.0 ± 6.0		
$\lambda_{\rm bs}(^\circ)$	162.0 ± 9.0			$\lambda_{\rm bs}(^\circ)$	154.0 ± 9.0		
$\Omega_{\rm h}$	9.90 ± 0.03			$\Omega_{\rm h}$	8.83 ± 0.03		
$\Omega_{\rm c}$	2.35 ± 0.02			$\Omega_{\rm c}$	2.35 ± 0.02		

Fixed parameters: $q = \mathcal{M}_{\rm c}/\mathcal{M}_{\rm h} = 0.25$ – mass ratio of the components; $T_{\rm c} = 7900$K – temperature of the less massive (cooler) donor; $F_{\rm c} = 1.0$ – filling factor for the critical Roche lobe of the donor; $f_{\rm c} = 1.00$ – non-synchronous rotation coefficients of the donor; $\beta_{\rm h,c} = 0.25$ – gravity-darkening coefficients of the components; $A_{\rm h,c} = 1.0$ – albedo coefficients of the components. *Notes*. n = number of observations; $\Sigma(\mathrm{O-C})^2$ = final sum of squares of residuals between observed (LCO) and synthetic (LCC) light curves; $\sigma_{\rm rms}$ = root mean square of the residuals; i = orbit inclination (in arc degrees); $F_{\rm d} = R_{\rm d}/R_{yc}$ = disc dimension factor (the ratio of the disc radius to the critical Roche lobe radius along y-axis); $T_{\rm d}$ = disc-edge temperature, $d_{\rm e}$, $\mathrm{d_c}$, - disc thicknesses (at the edge and at the centre of the disc, respectively) in the units of the distance between the components; $a_{\rm T}$ = disc temperature distribution coefficient; $f_{\rm h}$ = non-synchronous rotation coefficient of the more massive gainer (ratio between the rotational angular velocity and the synchronous rotational angular velocity); $F_{\rm h} = R_{\rm h}/R_{zc}$ = filling factor for the critical Roche lobe of the hotter, more massive gainer (ratio of the stellar polar radius to the critical non-synchronous Roche lobe radius along z-axis for a star in critical rotation regime, equal to 1 for critical rotation regime); $T_{\rm h}$ = temperature of the gainer; $A_{\rm hs,bs} = T_{\rm hs,bs}/T_{\rm d}$ = hot and bright spots' temperature coefficients; $\theta_{\rm hs,bs}$ and $\lambda_{\rm hs,bs}$ = spots' angular dimensions and longitudes (in arc degrees); $\theta_{\rm rad}$ = angle between the line perpendicular to the local disc edge surface and the direction of the HS maximum radiation; $\Omega_{\rm h,c}$ = dimensionless surface potentials of the hotter gainer and cooler donor; $\mathcal{M}_{\rm h,c}(\mathcal{M}_\odot)$, $\mathcal{R}_{\rm h,c}(\mathrm{R}_\odot)$ = stellar masses and mean radii of stars in solar units; $\log g_{\rm h,c}$ = logarithm (base 10) of the system components effective gravity; $M^{\rm h,c}_{\rm bol}$ = absolute stellar bolometric magnitudes, $a_{\rm orb}$ ($\mathrm{R}_\odot$), $\mathcal{R}_{\rm d}(\mathrm{R}_\odot)$, $d_{\rm e}(\mathrm{R}_\odot)$, $d_{\rm c}(R_\odot)$ = orbital semi-major axis, disc radius and disc thicknesses at its edge and centre, respectively, given in solar units.

rough approximation of the hot line which forms at the edge of the gas stream between the components (Bisikalo et al. 2003). Although including the HS region into the model significantly improves the fit, it cannot explain the light-curve asymmetry completely. By introducing one additional BS, larger than the HS and located on the disc edge at $\lambda_{\rm bs} \approx 160^\circ$, the fit becomes much better.

4 DISCUSSION

4.1 Disc formation

In a semi-detached system with the donor transferring matter on to the gainer through an accretion stream, the stream has a distance of closest approach $r_{\rm min}$ from the centre of the gainer, given approximately by

$$\frac{r_{\rm min}}{a} = 0.0488 q^{-0.464} \qquad (3)$$

(Lubow & Shu 1975). Using $q = 0.25$ we obtain $r_{\rm min} = 0.093\ a$, comparable to the gainer radius ($0.125 \pm 0.046\ a$). The fact that our light-curve model shows a relatively large disc around the gainer indicates that: (i) the stream in principle hits the gainer that rapidly reaches critical rotation (Packet 1981), it cannot accrete additional mass and a disc is built around the star or (ii) the gainer radius is smaller than $r_{\rm min}$ and a disc is formed naturally. At present, uncertainties in q and $R_{\rm h}$ do not allow us to select between these mutually exclusive alternatives.

4.2 On the cause for the long cycle

It is notable that the model containing the circumprimary disc fits very well the orbital light curve *through the whole long cycle*. This fact suggests that the optically thick disc does not participate in the long cycle, at least that part of the disc responsible for the orbital photometric variability. We conclude that the long cycle is produced by an additional variable and non-eclipsed emitting structure, a fourth light in the system. In addition, the fact that this fourth light is redder at long maximum and bluer at minimum places strong constrains on the possible cause for the long-cycle variability.

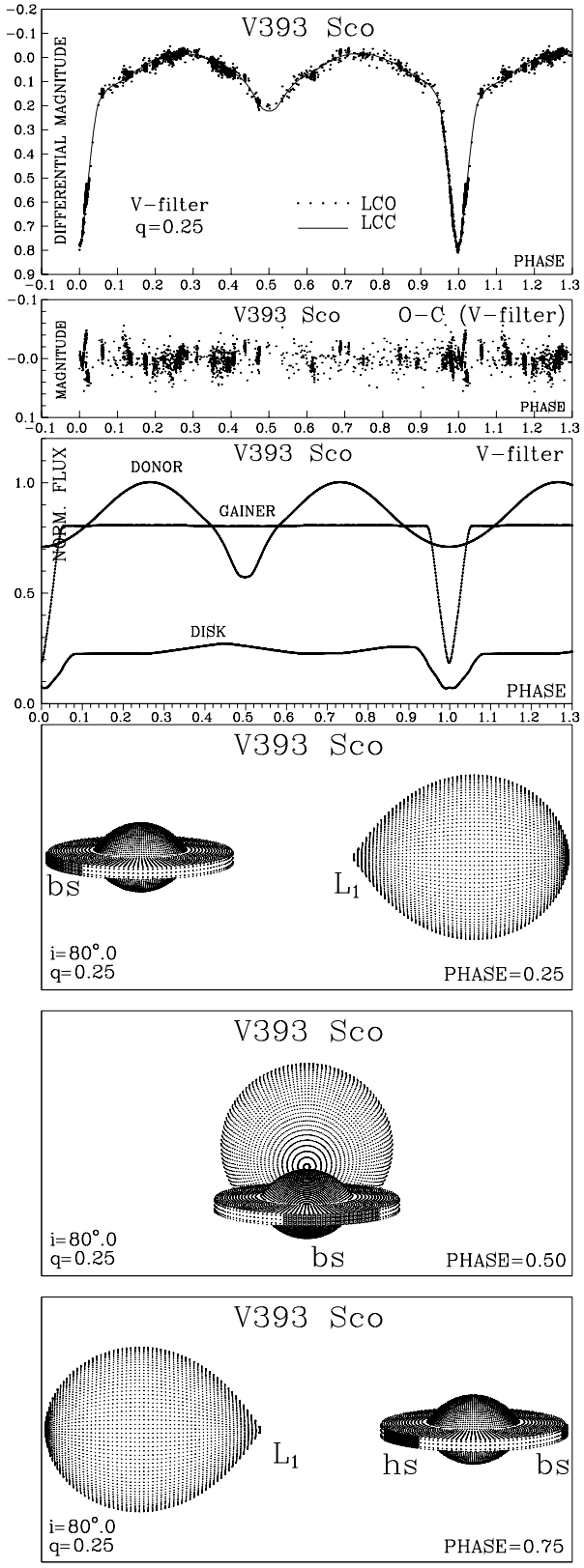

Figure 2. Observed (LCO) and synthetic (LCC) light curves of V 393 Sco obtained by analysing photometric observations; final O–C residuals between the observed and optimum synthetic light curves; fluxes of donor, gainer and of the disc, normalized to the donor flux at phase 0.25; the views of the optimal model at orbital phases 0.25, 0.50 and 0.75, obtained with parameters estimated by the light-curve analysis.

In principle, it is possible that the long minimum is due to obscuration of the system by ejected material through the equatorial plane, as suggested by M10's observations. This possibility is not supported by our observations, since it should produce a white (opaque material) or red (gas producing reddening in the line of sight and free–free emission outside the line of sight) minimum. In contrast, our observations indicate that the system when brighter is redder, a fact consistent with free–free emission in non-obscured ejected circumbinary material. If this material is not ejected in the orbital plane at long maximum, then it is ejected at higher latitudes. In this sense the inferred variable emitting structure is reminiscent of the jets found in β Lyr (Harmanec et al. 1996; Harmanec 2002).

This interpretation conflicts with the M10 suggestion that mass loss occurs in the equatorial plane. That position was based on the non-variability of UV spectral features through the long cycle and the evidence for mass flows through the L3 point. However, only few UV spectra were available for analysis, and it is possible that the putative variability was hidden by additional orbital variability, or alternatively, the long-cycle variability disappears at UV wavelengths. Much more well-sampled UV spectra are needed to illuminate this point. In addition, the inferred mass loss through L3 around secondary eclipse is still compatible with vertical outflows. Furthermore, UV lines *do* show evidence for such high latitude outflows (M10).

4.3 Mass transfer and mass loss

In this section we calculate the mass transfer rate ($\dot{M}$) for Model A using several approaches. The radial temperature structure of a steady-state accretion disc is given by

$$T(r) = T_0 \left[\frac{r}{R_\mathrm{h}}\right]^{-3/4} \left[1 - \left[\frac{R_\mathrm{h}}{r}\right]^{1/2}\right]^{1/4} \quad (4)$$

where

$$T_0 = \left[\frac{3GM_\mathrm{h}\dot{M}}{8\pi\sigma R_\mathrm{h}^3}\right]^{1/4} \quad (5)$$

where G is the gravitational constant and σ the Stephan–Boltzman constant (e.g. Warner 1995). From the above expressions and using the parameters given in Table 2 and $T = 8600$ K (the temperature in the disc outer edge) we obtain $\dot{M} = 3.74 \times 10^{-5}$ M$_\odot$ yr^{-1}.

Let us use the formula given by Smak (1989) for the geometrical thickness H of an α-disc at the density level of 10^{-10} g cm^{-3}:

$$\frac{H}{R_\mathrm{d}} \approx 0.07 \left[\dot{M}_{18}\left(1 - \left(\frac{R_\mathrm{h}}{R_\mathrm{d}}\right)^{0.5}\right)\right]^{0.18} \quad (6)$$

where $\dot{M}_{18}$ is the mass accretion rate in units of 10^{18} g s^{-1}. Using the average between d_e and d_c as the value for H, we found $\dot{M} = 7.97 \times 10^{-6}$ M$_\odot$ yr^{-1}.

Now we assume that at $\Phi_o = 0.25$ the system magnitude is $V = 7.609$ (Table 4). From the light-curve model the disc flux contribution at this phase is 10 per cent. Considering the reddening $E(B-V) = 0.13$ and a distance of 523 pc (M10) we obtain $V^\mathrm{disc} = 9.68$ and $M_V^\mathrm{disc} = 1.09$. Using the bolometric correction BC $= -1.50$ for $T = 17\,000$ K, $\log g = 3.0$, and $Z = Z_\odot$ (Lanz & Hubeny 2007) we obtain $M_\mathrm{bol}^\mathrm{disc} = -0.41$ corresponding to 115 L$_\odot$. If this luminosity is powered by accretion, then

$$L^\mathrm{disc} = \frac{GM_\mathrm{h}\dot{M}}{2R_\mathrm{h}} \quad (7)$$

(e.g. Warner 1995). Using the above equation we derive $\dot{M} = 4.15 \times 10^{-6}$ M$_\odot$ yr^{-1}.

If the DPV long cycles are due to recurrent episodes of systemic mass loss as suggested by Mennickent et al. (2008), and assuming no mass accumulation around the gainer in the long term, then $\Delta M = \dot{M}\ P_{\rm long}$ are ejected from the system every long cycle. For the $\dot{M}$ values given above this means that ΔM between 5.4×10^{-5} and 2.9×10^{-6} $M_\odot$ are ejected in every cycle. We find that in an accretion-powered system, the amount of mass lost in every long cycle is not minor and should affect the system evolution considerably.

If the system loses mass due to a spherically symmetric wind that does not interact with the companion, then the orbital period changes by (e.g. Hilditch 2001)

$$\frac{\dot{P}_o}{P_o} = \frac{-2\dot{M}_{\rm h}}{M_{\rm h} + M_{\rm c}}. \quad (8)$$

Using our stellar masses and estimates for the mass loss rate given above we find changes in the orbital period of 1 to 10 s per year, easily detectable with the current astronomical instrumentation. The fact that this variability is not observed argues against an accretion disc whose luminosity is driven by viscosity but in favour of an extended photosphere radiating by reprocessed stellar radiation. This view is also supported by other evidence presented later in the next section.

4.4 Evolutionary stage of V 393 Scorpii

The comparison of the stellar parameters with predictions of evolutionary models for single stars with solar metallicity indicates: (i) the donor is significantly inflated appearing as an overluminous object for its mass and (ii) the gainer is underluminous and underheated for the given mass (Fig. 3). The inflated cooler star is expected in a semi-detached interacting binary with an evolved donor whereas the underluminous hotter star can reveal the presence of a massive circumprimary disc. In fact, the loci occupied by the 7.8 $M_\odot$ gainer in the Hertzsprung–Russell diagram corresponds to a slightly evolved 6 $M_\odot$ star. The figure $R_{\rm h} = 4.4$ $R_\odot$ is also compatible with a 6 $M_\odot$ star. This could be possible if a 2 $M_\odot$ optically thick disc

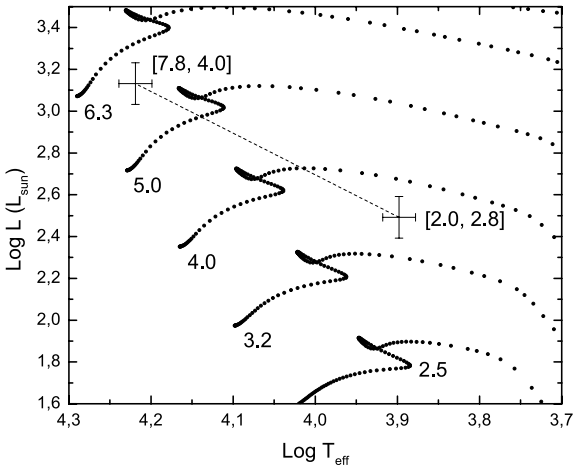

Figure 3. Evolutionary tracks for single stars with solar metallicity (Claret 2004) and the position for the stellar components of V 393 Sco. Derived masses and log g values are given between parentheses. The evolutionary tracks are labelled with initial masses.

surrounds the gainer. In other words, in this view, our dynamical mass is overestimated by the presence of a massive disc.[4]

The average disc electron number density can be estimated from

$$n_{\rm e} = \frac{M_{\rm disc}}{\pi H m_{\rm e} \left(R_{\rm d}^2 - R_{\rm h}^2\right)}. \quad (9)$$

Using the values given in Table 2 and $M_{\rm disc} = 2\ M_\odot$ we derive $n_{\rm e} = 3.2 \times 10^{25}$ cm^{-3}. This density is much larger than that found in a normal B-type photosphere and comparable with densities found in the stellar interior.

An alternative explanation involving a less massive disc is that the gainer light is in some way obscured by the presence of the high latitude wind detected in the UV producing a smaller effective temperature and luminosity. Whereas the hypothesis of a massive disc explains the small $R_{\rm h}$, the obscuration effect does not.

The hypothesis of a self-gravitating massive disc (0.5 $M_\odot$) for the DPV-related system β Lyr was considered by Wilson & Terrell (1992) but critiqued by Hubeny, Harmanec & Shore (1994) who pointed out that a massive-disc model requires unrealistically low viscosity, i.e. a large Reynolds number, and is likely to be dynamically unstable. All these authors assumed accretion-powered discs in their calculations, leaving the door open for a structure with a different mechanism for energy generation. Further theoretical work is necessary to explore alternative physical scenarios for massive discs around normal stars more deeply.

Now we consider predictions of binary evolution models including epochs of systemic mass loss. We inspected the 561 conservative and non-conservative evolutionary tracks by van Rensbergen et al. (2008) available at the Center de Données Stellaires (CDS) looking for the best match for the system parameters found for V 393 Sco. Models with strong and weak tidal interaction were studied, although only the latter ones should allow critical rotation of the gainer. A multi-parametric fit was made with the synthetic ($S_{i,j,k}$) and observed (O_k) stellar parameters mass, temperature, luminosity and radii, and the orbital period, where i (from 1 to 561) indicates the synthetic model, j the time t_j and k (from 1 to 9) the stellar or orbital parameter. Non-adjusted parameters were mass-loss rate, Roche lobe radii, chemical composition, fraction of accreted mass lost by the system and age. For every synthetic model i we calculated the quantity $\chi^2_{i,j}$ at every t_j defined by

$$\chi^2_{i,j} \equiv (1/N)\Sigma_k w_k[(S_{i,j,k} - O_k)/O_k]^2 \quad (10)$$

where N is the normalization factor and w_k the statistical weight of the parameter O_k, calculated as

$$w_k = \sqrt{O_k/\epsilon(O_k)} \quad (11)$$

where $\epsilon(O_k)$ is the error associated with the observable O_k. The model with the minimum χ^2 corresponds to the model with the best evolutionary history of V 393 Sco. The absolute minimum $\chi^2_{\rm min}$ identifies the age of the system along with the theoretical stellar and orbital parameters. The high accuracy of the orbital period dominates the search for the best solution in a single evolutionary track, but the others parameters play a role when comparing tracks corresponding to different initial stellar masses.

We find the absolute χ^2 minimum in the weak interaction model with initial masses of 6 and 3.6 $M_\odot$ and initial orbital period of 3 d. This model starts Roche lobe overflow at about the same time

[4] The DPV AU Mon suffers from the same problem. Considering $M_1 = 7$ $M_\odot$, $\log T_{\rm h} = 4.20$ and $\log L_{\rm h} = 3.17$ found by Djurašević et al. (2010) the gainer turns to be underluminous.

Table 3. The parameters of the van Rensbergen et al. (2008) model that best fits the V 393 Sco data. The hydrogen and helium core mass fractions (X_c and Y_c) are given for the cool and hot star.

Quantity	Value	Quantity	Value
Age	7.00E7 yr	Period	7.713 d
M_c	2.11 $M_\odot$	M_h	7.49 $M_\odot$
$\dot{M}_c$	−9.47E-9 $M_\odot$ yr^{-1}	$\dot{M}_h$	9.47E-9 $M_\odot$ yr^{-1}
log T_c	3.92 K	log T_h	4.32 K
log L_c	2.61 $L_\odot$	log L_h	3.39 $L_\odot$
R_c	9.55 $R_\odot$	R_h	3.79 $R_\odot$
X_{cc}	0.05	X_{ch}	0.63
Y_{cc}	0.93	Y_{ch}	0.35

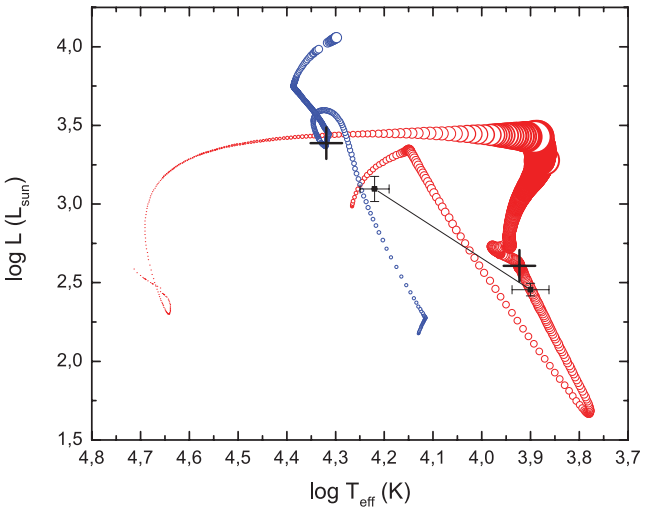

Figure 4. Evolutionary tracks for the binary star model from van Rensbergen et al. (2008) that best fit the data. Donor (right track) and gainer (left track) evolutionary paths are shown, along with the observations for V 393 Scorpii (with error bars and connecting line). The best fit is reached at the time corresponding to the model indicated by large crosses, that is characterized in Table 3. The mismatch for the primary is discussed in the text. Stellar sizes are proportional to the circle diameters.

that core hydrogen burning ends, so it is a borderline Case A/B (thanks to Nicki Mennekens for this insight). The averages of their parameters are shown in Table 3.

The corresponding evolutionary tracks for the primary and secondary stars are shown in Fig. 4, along with the position for the best model for V 393 Sco. We observe a relatively good match for the donor star parameters but a mismatch with the gainer temperature and luminosity. The higher stellar temperature and luminosity indicated by the model could indicate that in practice the gainer has not accreted all the transferred mass but part of the mass has been accumulated in a massive optically thick surrounding disc. Consequently, lower temperatures and luminosities are observed for the gainer, those corresponding to the actual stellar mass. This conclusion is consistent with our previous discussion and was obtained in an independent way.

The best fit also indicates that V 393 Sco is found after a burst of mass transfer, the gainer having received 4 $M_\odot$ in a rapid burst lasting 400 000 years. The donor is an inflated ($R_c = 9.6\ R_\odot$) and evolved 2 $M_\odot$ star with its core consisting of 93 per cent of helium. According to the best model the system has now an age of 7.00×10^7 yr and $\dot{M} = 9.47 \times 10^{-9}\ M_\odot\ yr^{-1}$ (Fig. 5).

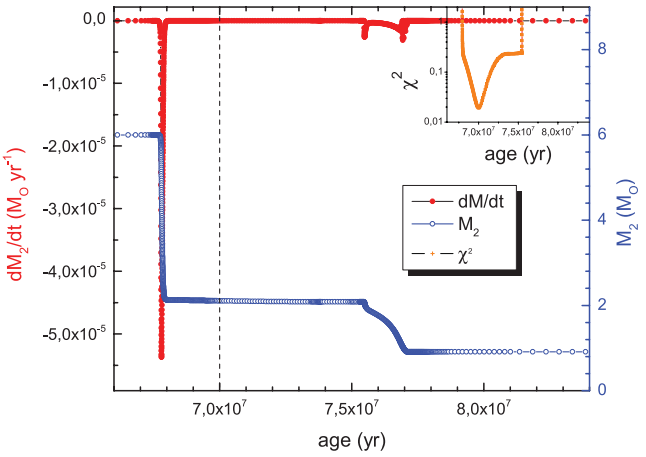

Figure 5. $\dot{M}_2$ (upper curve) and M_2 for the best evolutionary model. The vertical dashed line indicates the position for the best model. χ^2 is shown in the inset graph.

We notice that the mass transfer rate derived from model fitting is much smaller than those derived in Section 4.3. This could indicate that: (i) $\dot{M}$ values are still not well reproduced by the models or (ii) basic assumptions of Section 4.1 are invalid, like accretion-powered disc luminosity and the hypothesis of a steady-state accretion disc. The fact that we obtain different values of $\dot{M}$ using the accretion-powered hypothesis and that we do not observe orbital period changes argues for the second alternative. If viscous dissipation in an accretion disc is not the source of disc luminosity then other mechanisms should be invoked, like shocks produced in impact regions or photoionization of circumstellar gas and recombination of high-energy photons produced in hot regions. If the disc is considered an extension of the gainer photosphere, it should fit its temperature at the inner region but should show cooler temperatures at the outer regions, as indicated by equation (2). In this case we expect the spectral energy distribution be characterized by thermal radiation from an optically thick disc in thermal contact with the hotter star. In this view, it is the gainer that maintains the hot disc, not viscous dissipation.

The low $\dot{M}$ model imposes certain problems for the accretion-powered disc, but explains the absence of measured orbital period changes. On the other hand, it is not impossible to assume that low $\dot{M}$ values maintain the long cycle. If we assume $\dot{M} = 9 \times 10^{-9}$ $M_\odot\ yr^{-1}$ then 6.2×10^{-9} $M_\odot$ are ejected in steady state in a long cycle. The low $\dot{M}$ solution implies that V 393 Sco is in a relatively long-lasting evolutionary stage compared with the previous rapid mass transfer rate stage. This implies that a relatively large number of systems should be found showing the DPV phenomenon, as actually observed.

If we require the best-fitting model to match the high $\dot{M}$ value then we should look at the end of the rapid mass transfer burst (younger system with age 6.8×10^7 yr) or at the beginning of the following mass transfer event (older system with age 7.55×10^7 yr; Fig. 5). In both cases we can get $\dot{M}$ values of the order of 10^{-6} $M_\odot\ yr^{-1}$. However, these models have larger χ^2 values than the preferred model by a factor of 10. In both cases, our conclusion that a massive structure surrounds the gainer remains unaltered.

4.5 Double periodic variables in the Milky Way

We performed a search for Galactic DPVs in the ASAS catalogue using the software described in Section 3. Light curves were

Table 4. DPVs in the Milky Way detected from the analysis of the ASAS data base. Remarks are from SIMBAD (http://simbad.u-strasbg.fr/simbad/) except for V 393 Sco that are from this paper.

Names			RA(2000)	Dec. (2000)	P_{orb}	P_{long}	TYCHO-2		Remarks
HD	TYCHO	GCVS			(d)	(d)	B_T	V_T	
50526	161-1014-1	–	06:54:02.04	+06:48:48.5	6.7015	191.7	8.342	8.244	B9
50846	54801-1012-1	AU Mon	06:54:54.71	−01:22:32.9	11.1132	419.0	8.453	8.432	Ecl B3V+F8IIIe
–	5978-472-1	–	07:26:41.41	−22:08:53.7	8.2962	311.0	10.641	10.585	–
–	5985-958-1	–	07:44:15.30	−17:58:45.6	7.4062	229.5	10.713	10.641	–
–	8175-333-1	DQ Vel	09:30:34.22	−50:11:54.0	6.0833	188.0	11.473	10.977	Ecl
90834	–	–	10:27:41.61	−59:17:04.9	6.8148	230.7	9.591	9.500	B5III/IVe
135938	8695-2281-1	–	15:20:08.44	−53:45:46.5	6.6477	231.2	9.470	9.267	B5/B6IVp
–	8708-412-1	GK Nor	15:34:50.92	−58:23:59.1	6.5397	221.0	11.646	11.275	Ecl
328568	8325-3366-1	LP Ara	16:40:01.78	−46:39:34.9	8.5331	274.0	10.541	10.243	Ecl B8
161741	7385-1101-1	V 393 Sco	17:48:47.60	−35:03:25.6	7.7126	251.7	7.748	7.609	Ecl B4V/A7III
170582	5703-2382-1	–	18:30:47.53	−14:47:27.8	16.872	536.0	10.150	9.711	A3-A9

Table 5. Galactic hot emission-line binaries with cyclic long-term brightness changes (Desmet et al. 2010). P_{th} is the predicted long period according to equation (12). References for the spectral types are given.

Names			RA (2000)	Dec. (2000)	P_{orb}	P_{long}	P_{th}	Remarks
HD	TYCHO	GCVS			(d)	(d)	(d)	
–	4313-258-1	RX Cas	03:07:45.75	+67:34:38.6	32.312	516	1057	A5III+G3III; Strupat (1987)
174237	3918-1829-1	CX Dra	18:46:43.09	+52:59:16.7	6.696	130–180	219	B2.5V+F5III; Simon (1996)
174638	2642-2929-1	β Lyr	18:50:04.80	+33:21:45.6	12.94	282.4	423	B8epII+B6.5; Budding et al. (2004)
216200	3223-3619-1	V360 Lac	22:50:21.77	+41:57:12.2	10.085	322.2	330	Be+F; Linnell et al. (2006)

inspected for the presence of two periodicities. We found the 11 systems shown in Table 4 (see also Mennickent & Kołaczkowski 2009; Michalska et al. 2010, for previous reports on this investigation). Two of our detected DPVs were previously catalogued as Algol-type variables with additional long-term variability, viz. AU Mon and V393 Sco. The lack of dedicated stellar variability surveys in our Galaxy probably explains why the long photometric variability of many of these DPVs remained undetected for a long time. In Table 5 we also show those Galactic hot emission-line binaries with cyclic long-term brightness changes reported by Desmet et al. (2010, their table 10).

The hallmark of the DPV phenomenon, i.e. the correlation between the orbital and the long cycle, is shown in Fig. 6. V 393 Sco fits very well the general tendency. However, two of the objects listed by Desmet et al. (2010), namely β Lyr and RX Cas, clearly deviate from it. Excluding these two objects, the best linear fit for the remaining 13 systems is

$$P_{\rm long} = 32.7(9) P_o. \qquad (12)$$

This relation is comparable to previous relationships found for Large Magellanic Cloud (LMC) and Small Magellanic Cloud (SMC) DPVs, with respective coefficients 33.1 and 32.4 (Mennickent et al. 2005; Desmet et al. 2010).

According to this relationship, the predicted long period for β Lyr is about 423 d, 1.50 times longer than the reported 282 d, and for RX Cas is 1057 d, i.e. 2.05 times longer than reported. The commensurability of predicted and observed periods is notable. In order to investigate if the expected 423 d periodicity is present in the β Lyr photometry, we removed the orbital variability from the V-band light curve kindly provided by Dr. Harmanec and searched for additional frequencies. The residual periodogram shows the already known periods of 282 and 356 d but only a very small peak in 426 d. Residuals folded with this period show a very noisy diagram.

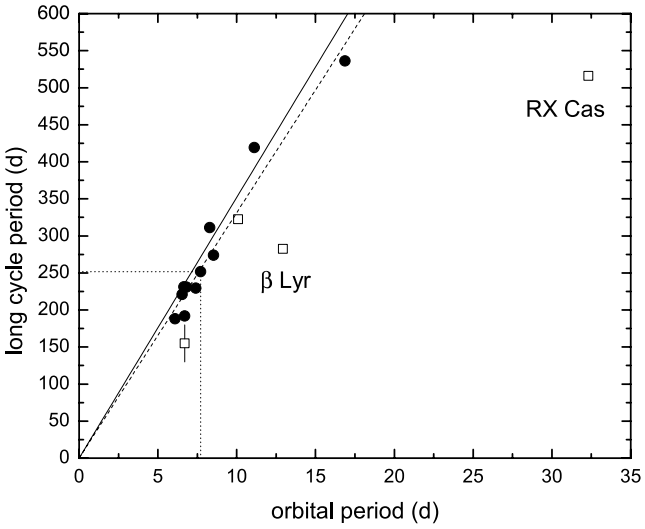

Figure 6. The DPVs listed in Table 4 (solid dots) and the hot emission-line binaries with cyclic long-term brightness changes listed in Table 5 (open squares). The upper and lower lines represent the best fit for 30 SMC DPVs (Mennickent et al. 2003) and 125 LMC DPVs (Poleski et al. 2010). The position of V 393 Scorpii is indicated by dotted lines.

It is possible that a different evolutionary stage explains the position of the outliers β Lyr and RX Cas in Fig. 6. These objects could still be inside the burst of mass transfer illustrated in Fig. 5, while DPVs should already have passed this stage. In favour of this interpretation is the fact that orbital period changes have been detected in β Lyr and RX Cas and interpreted as due to very large mass transfer rates ($\sim 10^{-5}$ $M_\odot$ yr^{-1}). However, orbital period changes have not been reported in DPVs.

5 CONCLUSIONS

In this paper we have modelled the *orbital* light curve of the intermediate-mass interacting binary V 393 Sco to obtain stellar and system parameters. We also disentangled the long-term light curve at optical and infrared photometric bands. We have found insights on the system evolutionary stage and long-cycle nature. The main results of our research are as follows.

(i) The orbital period change, if present, is shorter than 0.5 s per year.

(ii) The long-term light curves are characterized by a smooth oscillation in a time-scale of 253 d with larger amplitudes in redder bandpasses.

(iii) The best fit to the orbital light curve requires a non-stellar component that was modelled with an optically thick disc model. The disc radius is about half of the Roche lobe radius of the gainer and two BSs are required to fit the observations.

(iv) We found the stellar and system parameters that best match the observations, which are given in Table 2 along with parameters for the disc and the BSs.

(v) The stability of the orbital light curve suggests that the stellar + disc configuration remains stable during the long cycle. Variability of the optically thick disc is not the main source for long cycle.

(vi) Therefore and in order to fit the redder colour at long maximum, we argue that the long cycle is produced by free–free emission in a variable structure, probably visible perpendicular to the orbital plane, something reminiscent of the jets found in β Lyr (Harmanec et al. 1996). The suggestion of equatorial mass loss as the cause of the long cycle by M10 is probably biased by detection of equatorial outflows not necessarily related to the long cycle.

(vii) A comparison with published evolutionary tracks provides an estimate for the age of the system, namely $\log t = 7 \times 10^7$ yr. We find the system after a mass exchange episode, where 4 $M_\odot$ were transferred from the donor to the gainer in a period of 400 000 yr.

(viii) The evolutionary model with initial stellar masses of 6 and 3.6 $M_\odot$ reproduces relatively well the present donor parameters and orbital period, but overestimates the gainer temperature and luminosity, a fact that could be ascribed to the optically thick disc not considered in the evolutionary tracks. In order to explain these features, we argue that part of the mass, maybe up to 2 $M_\odot$, has not been accreted by the gainer, but remains in the *massive* optically thick disc.

(ix) We find a discrepancy between values of $\dot{M}$ derived from theoretical model fitting of observationally derived parameters and those derived from accretion-theory analysis of observationally derived parameters, the former being smaller by 2 orders of magnitude. If the optically thick disc is a representation of a massive disc-like pseudo-photosphere, then its luminosity could not be accretion-driven. The constancy of the orbital period supports the view that the disc luminosity is not driven by viscosity, but probably by reprocessed stellar radiation.

(x) We present the results of our search for Galactic DPVs and make a comparison with hot emission-line binaries with cyclic long-term brightness changes. 13 Galactic DPVs show a similar correlation between P_o and $P_{\rm long}$ to that observed in LMC and SMC DPVs. The systems β Lyr and RX Cas deviate from this tendency. These systems could be in an earlier evolutionary stage compared with DPVs.

ACKNOWLEDGMENTS

We thank the anonymous referee for useful comments on the first version of this manuscript. REM acknowledges support by Fondecyt grant 1070705, 1110347, the Chilean Center for Astrophysics FONDAP 15010003 and from the BASAL Centro de Astrofisica y Tecnologias Afines (CATA) PFB–06/2007. GD acknowledges the financial support from the Ministry of Education and Science of the Republic of Serbia through the project 176004 'Stellar physics'. We thank Nicki Mennekens for conversations about the evolutionary models discussed in this article and Dr. P. Harmanec for kindly providing the light curve of β Lyr for its inspection.

REFERENCES

Allard C., Lupton R. H., 1998, ApJ, 503, 325
Bisikalo D. V., Boyarchuk A. A., Kaigorodov P. V., Kuznetsov O. A., 2003, Astron. Rep., 47, 809
Budding E., Erdem A., Cicek C., Bulut I., Soydugan F., Soydugan E., Bakis V., Demircan O., 2004, VizieR On-line Data Catalog, 341, 70263
Claret A., 2004, A&A, 424, 919
de Mink S. E., Pols O. R., Glebbeek E., 2007, in Stancliffe R. J., Dewi J., Houdek G., Martin R. G., Tout C. A., eds, AIP Conf. Ser. Vol. 948, Unsolved Problems in Stellar Physics: A Conference in Honor of Douglas Gough. Am. Inst. Phys., New York, p. 321
Desmet M. et al., 2010, MNRAS, 401, 418
Djurašević G., 1992, Ap&SS, 196, 267
Djurašević G., 1996, Ap&SS, 240, 317
Djurašević G., Latković O., Vince I., Cséki A., 2010, MNRAS, 409, 329
Harmanec P., 2002, Astron. Nachr., 323, 87
Harmanec P. et al., 1996, A&A, 312, 879
Heemskerk M. H. M., 1994, A&A, 288, 807
Hilditch R. W., 2001, An Introduction to Close Binary Stars. Cambridge Univ. Press, Cambridge
Hubeny I., Harmanec P., Shore S. N., 1994, A&A, 289, 411
Kreiner J. M., 2004, Acta Astron., 54, 207
Lanz T., Hubeny I., 2007, ApJS, 169, 83
Linnell A. P. et al., 2006, A&A, 455, 1037
Lubow S. H., Shu F. H., 1975, ApJ, 198, 383
Mennickent R. E., Kołaczkowski Z., 2009, Rev. Mex. Astron. Astrofs. Ser. Conf., 35, 166
Mennickent R., Kołaczkowski Z., 2010, in Andrej P., Miloslav Z., eds, ASP Conf. Ser. Vol. 435, Binaries – Key to Comprehension of the Universe. Astron. Soc. Pac., San Francisco, p. 283
Mennickent R. E., Pietrzyński G., Diaz M., Gieren W., 2003, A&A, 399, L47
Mennickent R. E., Assmann P., Pietrzyński G., Gieren W., 2005, in Sterken C., ed., ASP Conf. Ser. Vol. 335, The Light-Time Effect in Astrophysics. Astron. Soc. Pac., San Francisco, p. 129
Mennickent R. E., Kołaczkowski Z., Michalska G., Pietrzyński G., Gallardo R., Cidale L., Granada A., Gieren W., 2008, MNRAS, 389, 1605
Mennickent R. E., Kołaczkowski Z., Graczyk D., Ojeda J., 2010, MNRAS, 405, 1947 (M10)
Michalska G., Mennickent R. E., Kołaczkowski Z., Djurašević G., 2010, in Andrej P., Miloslav Z., eds, ASP Conf. Ser. Vol. 435, Binaries – Key to Comprehension of the Universe. Astron. Soc. Pac., San Francisco, p. 357
Packet W., 1981, A&A, 102, 17
Peters G. J., 2001, in Vanbeveren D., ed., Astrophysics and Space Science Library (ASSL), Vol. 264, Proc. Influence of Binaries on Stellar Population Studies. Kluwer, Dordrecht, p. 79
Peters G. J., Polidan R. S., 1984, ApJ, 283, 745
Pilecki B., Szczygiel D. M., 2007, Int. Bull. Var. Stars, 5768, 1
Pojmanski G., 1997, Acta Astron., 47, 467
Poleski R., Soszyński I., Udalski A., Szymański M. K., Kubiak M., Pietrzyński G., Wyrzykowski Ł., Ulaczyk K., 2010, Acta Astron., 60, 179

Simon V., 1996, A&A, 308, 799
Smak J., 1989, Space Sci. Rev., 50, 107
Stellingwerf R. F., 1978, ApJ, 224, 953
Strupat W., 1987, A&A, 185, 150
van Rensbergen W., De Greve J. P., De Loore C., Mennekens N., 2008, VizieR On-line Data Catalog, 348, 71129
von Zeipel H., 1924, MNRAS, 84, 702
Warner B., 1995, in Andrew K., Douglas L., Stephen M., Jim P., Martin W., eds, Cataclysmic Variable Stars. Camb. Astrophys. Ser. Vol. 28. Cambridge Univ. Press, Cambridge
Wilson R. E., Terrell D., 1992, Ann. New York Acad. Sci., 675, 65
Zola S., 1991, Acta Astron., 41, 213

This paper has been typeset from a TEX/LATEX file prepared by the author.